# Exergy analysis of surface heat exchangers for aircraft engine applications

Edoardo Paladini, Alexandre Couilleaux, Matteo Gelain, Nicolas Sirvin, Ilias Petropoulos

Association Aéronautique et Astronautique de France

*58th 3AF International Conference on Applied Aerodynamics*
*27 – 29 March 2024, Orléans - France*

**AERO2024-17**

# Exergy analysis of surface heat exchangers for aircraft engine applications

**E. Paladini[(1)], A. Couilleaux[(1)], M. Gelain[(1)], N. Sirvin[(1)], I. Petropoulos[(2)]**
[(1)] *Safran Aircraft Engines, Rond-Point René Ravaud - Réau, 77550 Moissy-Cramayel, France*
*email: edoardo.paladini@safrangroup.fr*
[(2)] *ONERA, 8 rue des Vertugadins, 92190 Meudon, France email: Ilias.petropoulos@onera.fr*

## ABSTRACT

The objective of the present paper is to present analyses of Surface Air-Cooled Oil-Cooler (SACOC) heat exchanger devices using exergy-based flow field analysis, which is an innovative assessment method in an industrial environment. In the frame of the DGAC research project IDEFFIX, Safran Aircraft Engines worked conjunctly with ONERA to test FFX (ONERA software for the analysis of CFD flow solutions) on complex industrial configurations. This software is used for the aero-thermal performance assessment of these configurations based on a balance of exergy. This work aims at highlighting the benefit of the exergy approach in addition to classical assessment methodologies (based on a force balance, total pressure losses, …) and to open the way towards a more innovative and efficient design of heat exchangers and their integration in future civil aircraft engines.

## 1. INTRODUCTION

In the pursuit of enhancing the efficiency and performance of modern aircraft engines, the optimization of heat exchangers plays a central role. These components are critical in managing thermal energy within the engine system, influencing overall efficiency, emissions, and operational reliability. Surface Air-Cooled Oil-Cooler (SACOC) [1] heat exchangers are a technology that recently entered service on the aircraft engine fleet (CFM LEAP), with Safran Aircraft Engines having been strongly involved in their development over the past years. The new aircraft engine challenge towards aeronautical de-carbonation involves architectures which are drastically different from current-generation "classical" aircraft engines [2]. These increase the requirement of heat exchange while the cold source (i.e. the fuel) is reducing. On the one hand, cooling requirements of this heat exchange are essential to ensure operational safety and consistent performance. On the other hand, the integration of heat exchangers introduces aerodynamic performance losses. A fine balance between these two aspects is therefore key for the optimal design of heat exchangers aimed at the future generation of aircraft.

SACOC devices are currently the reference technology, characterized by their minimal aerodynamic disruption to the flow [5]. While finned heat exchangers are not new, their behaviour in turbofan bypass flows has received limited attention. Previous works have analysed them in an isolated context, both numerically [6, 7] and experimentally [10, 11], but few studies in the literature have considered their integration into turbofan engines [8, 9]. Safran Aircraft Engines faces challenges in characterizing SACOC performance under realistic conditions. This leads to shortcomings of the design methodology of such devices in the industry because full-scale engine tests are costly and time-consuming, in turn making smaller-scale experimental tests and simulations necessary. Safran Aircraft Engines, at the forefront of aerospace engineering, collaborates with ONERA, leveraging their expertise in computational fluid dynamics (CFD) and aerodynamic performance analysis. In particular, within the project IDEFFIX (Industrial Development of Far-Field Exergy) [20], Safran Aircraft Engines worked in the application of the ONERA FFX analysis software on research configurations of industrial complexity. The collaboration between Safran Aircraft Engines and ONERA underscores a synergy between industrial expertise and cutting-edge research methodologies, aimed at addressing the multifaceted challenges of aerospace propulsion in the future generations of aircraft engines. Through this collaborative effort, we aim at elucidating the thermodynamic intricacies governing heat transfer processes and their interaction with aerodynamic flows within turbofan engine heat exchangers, ultimately paving the way for more efficient and sustainable propulsion systems.

This paper presents a comprehensive analysis of SACOC devices for aircraft engines, employing an exergy-based approach. Exergy (i.e. the potential for mechanical work extraction for a system in interaction with a reservoir) quantifies the maximum useful work obtainable from a system as it comes into equilibrium with its surroundings. This is used to form a balance which decomposes the exergy provided to or extracted from the fluid (by the propulsion or heat sources/sinks) into three main parts: the one consumed to produce effective thrust, the one that is theoretically convertible into work but is wasted and deposited to the freestream flow (e.g. jet kinetic energy), and finally the exergy dissipated due to irreversible phenomena (viscous effects, thermal mixing, shockwaves). The resulting balance is particularly adapted to the study of aero-thermal devices because it includes mechanical, compressible and thermal effects in the analysis. By the application of exergy-based flow field analysis over computational fluid dynamics (CFD) simulations, this study explores the intricate interplay between fluid dynamics and thermodynamics within heat exchanger systems in aircraft engines operating in transonic regime.

The study is structured in order to explore a range of heat exchanger configurations, progressing from simpler to more complex setups of interest at Safran Aircraft Engines. Beginning with an isolated SACOC fin in an infinitely-wide wind-tunnel test section, we conduct a parametric study to investigate the effects of varying boundary conditions (adiabatic, uniform isothermal, and based on aero-thermal coupling) on the flow around the SACOC fin. Moving to more realistic configurations, we examine a layout of sixteen SACOC fins positioned in a real wind-tunnel test section, in the wake of an Outlet Guide Vane (OGV). Finally, the study was extended to a case of realistic industrial complexity consisting in a fan/OGV followed by a SACOC integrated within a By-Pass Duct (BPD) and closely interacting with the OGV wake. This configuration is physically and numerically complex, involving parts of the computational domain computed either in a rotating or a fixed reference frame (connected by a mixing plane boundary condition), as well as viscous and thermal boundary conditions (resulting from an aero-thermal coupling) in an internal aerodynamics framework. This paper presents some of the main outcomes of exergy-based analyses across the aforementioned heat exchanger configurations of increasing complexity. We elucidate key insights gleaned from computational simulations and provide some perspectives on their implications for future aerospace engineering advancements. Additionally, we address the impact of thermal energy from heat exchangers on aircraft engine thermodynamics and explore its potential utilization in propulsion systems. The outline of the paper is as follows: Section 2 presents the exergy balance formulation; section 3 presents the results of the analysis in increasingly complex configurations ranging from an isolated SACOC and a sixteen-fin SACOC to the fan/OGV SACOC, and finally section 4 discusses the main conclusions of the study.

## 2. EXERGY DEFINITION & BALANCE FORMULATION

The concept of exergy in thermodynamics quantifies the maximum potential work obtainable from a system when interacting with a reservoir, which represents its thermodynamic dead state, through reversible processes. In the context of a perfect gas and without accounting for gravitational potential energy, the exergy can be mathematically expressed as follows [12]:

$$\chi = \delta e + p_\infty \delta (1/\rho) - T_\infty \delta s + \tfrac{1}{2} (\boldsymbol{V}-\boldsymbol{V}_\infty)^2 \qquad (1)$$

Here, ρ represents static density, $e$ stands for specific internal energy, T denotes static temperature, p denotes static pressure, and $s$ refers to specific entropy. The term $\delta(\bullet) = (\bullet)-(\bullet)_\infty$ represents the perturbation of a quantity concerning the reference state indicated by the subscript $\infty$.

The exergy balance within a fluid control volume around an aircraft or within an internal flow channel is essential for understanding energy transformations and losses. For external flows, the control volume boundaries may extend far upstream and laterally, with a user-prescribed downstream limit. This limit can vary to investigate different physical phenomena depending on the flow regions included in the control volume. The control volume may also rotate with the computational domain in rotating reference frame computations, thus remaining attached to the rotating fluid volume. Shockwave discontinuities may be present in the control volume. The system is thermodynamically open, exchanging mass, work, and heat across its boundaries.

The exergy balance can be expressed in different forms and thus provide insight tailored to the specific case under study. A commonly used compact form of the balance includes terms representing inflow of mechanical exergy via rotating surfaces (Xr) exergy due to throughflow models (Xtf), and exergy from conduction through non-adiabatic surfaces (Xq) [14].

$$\dot{\mathrm{X}}_r + \dot{\mathrm{X}}_{tf} + \dot{\mathrm{X}}_q = \dot{\mathrm{X}}_{tr} + \dot{\mathrm{X}}_m + \dot{\mathrm{X}}_{th} + \dot{\mathrm{A}}_\phi + \dot{\mathrm{A}}_{\nabla T} + \dot{\mathrm{A}}_w \qquad (2)$$

The right-hand side of the balance includes a term representing exergy converted to effective thrust (Xtr). The balance further breaks down the overall exergy flux into mechanical (Xm) and thermocompressible (Xth) components, accounting for kinetic energy perturbations, the rate of work of surface forces associated to the velocity perturbations and the flux of

the static portion of exergy itself. The remaining terms represent exergy dissipation due to irreversible effects such as viscous effects ($A_\Phi$), thermal mixing ($A_{\nabla T}$), and shockwaves ($A_w$). The balance highlights that not all of the exergy inflow is converted to effective thrust; some leaves as recoverable exergy (and will be eventually dissipated downstream) or is dissipated within the control volume by irreversible effects. This breakdown quantifies the impact of individual phenomena on the configuration's overall performance.

Specific figures of merit can be derived from the exergy balance, tailored to the performance analysis of the system under study. This detailed breakdown allows for adapting metrics to specific cases, considering factors like the mechanically-recoverable exergy flux [14,17]. Further studies have investigated the influence of the exergy balance on numerical error [15], or analysed the application of this particular balance and decomposition in turbomachinery cases [14].

## 3. SACOC CONFIGURATIONS

The three SACOC configurations analysed in the present work are those investigated in [1]. The SACOC consists of a sequence of staggered fins aligned with the main flow direction. The cooling mechanism involves the airflow passing through these fins, serving as the cold sink of the heat exchange. This airflow interacts with the surface of the fins, facilitating heat transfer with the fluid domain. In practical applications, such as those described in [5], the heat source of the exchanger is a sophisticated arrangement of channels and winglets positioned beneath the air-fins. These channels and winglets facilitate the flow of engine oil, serving as the hot source for the heat exchange process. In the present work, the thermal field on the surface of the heat exchanger fins in the CFD calculations is the result of an aero-thermal coupling between the elsA software [18] for the solution of fluid flow domain and the Zset software [13] for the solution of the solid domain. The simplicity of the first configuration studied, the isolated SACOC, allows the authors to test and compare aero-thermal coupling with isothermal and adiabatic boundary conditions in order to assess the impact of higher-fidelity boundary conditions in the CFD performance assessment of the configuration.

### 3.1. Isolated SACOC fin

The isolated SACOC fin configuration is the least complex case among the surface heat exchangers analysed in the present study. The lower geometrical complexity of this case (and therefore the lower CPU cost for the associated CFD studies) allows to easily investigate several numerical parameters and perform studies on the establishment of accurate numerical practice for such flows. The coupled aerothermal CFD computation was compared against others using isothermal (prescribed uniform wall temperature) and adiabatic computations to isolate and quantify the impact of thermal effects on the isolated SACOC configuration. The goal of this analysis is to qualitatively and quantitatively isolate the effect of introducing a SACOC in the channel flow, and therefore the mechanical, compressible and thermal effects associated to this device on engine thrust.

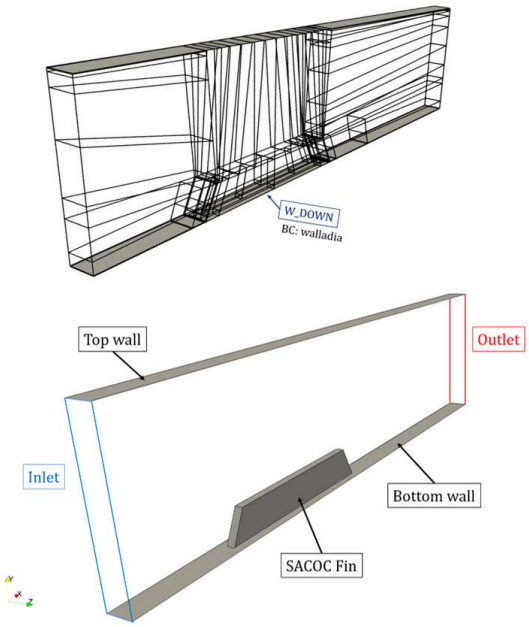


Figure 1: Mesh topology and boundary conditions of the reference duct calculation and isolated SACOC fin.

Fig. 1 shows a view of the topology of the isolated fin configuration, with a SACOC fin in a test channel and periodic boundary conditions in the transverse direction. The first investigation was carried out for the case where the non-adiabatic boundary condition on the SACOC fin surface is imposed through an aerothermal coupling. For all cases, the inlet boundary condition of the fluid volume is set by injecting a profile extracted from an engine computation (head-loaded profile), and the outlet is an imposed static pressure boundary condition. Fig. 2 shows a view of the flow field around the fin and the temperature field on its skin for this case.

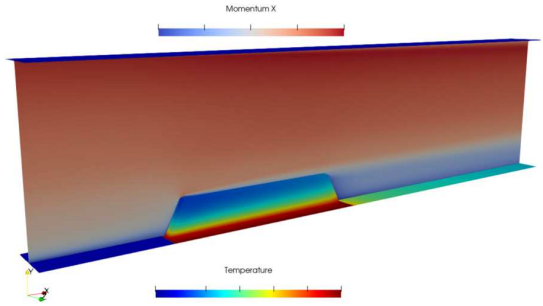


Figure 2: Isolated SACOC streamwise momentum component and temperature on the skin (aero-thermal coupling boundary condition).

This CFD solution was analysed using the FFX software in order to compute the exergy balance. The control volume for the analysis was defined considering a variation of its downstream transverse plane limit (position denoted as Xtp). This shows the variation of the exergy balance as the control volume extends downstream and thus includes additional reversible and irreversible flow phenomena.

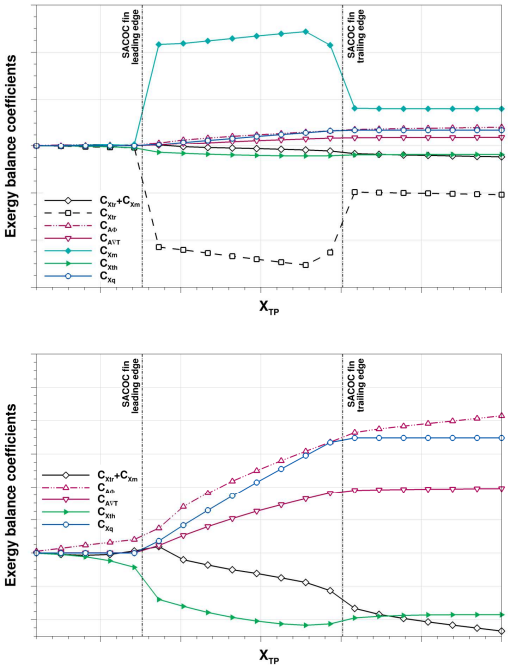


Figure 3: Overall evolution of the exergy balance for a variation of the control volume's downstream limit (top) and detail of specific components (bottom). Isolated SACOC fin case with aerothermal-coupling-based wall boundary condition.

The resulting variation of the exergy balance is shown in Fig. 3. The sum of the Xtr and Xm coefficients is often more representative in internal flows since, contrary to these two individual components, it is independent of the reference frame translation velocity [4]. As expected, this shows an overall decrease along the channel (i.e. the flux of mechanical exergy defined for a reference state at rest decreases). For the reference state velocity used in the present study, the overall streamwise force is shown to be that of an overall drag (negative Xtr component), which in terms of mechanical exergy flux is translated to notable variations along the fin. These are mainly a result of the rate of work of surface forces on the control volume boundary. The aforementioned two individual terms exhibit variations of a notably larger magnitude compared to terms associated to thermal effects. An overall decrease is also identified for the thermocompressible exergy outflow Xth. The same figure shows the introduction of thermal exergy (Xq) along the fin. This exergy inflow is found to have a rather linear trend in the central portion of the SACOC fin. Viscous anergy generation is shown to be significant along the complete length of the channel, but higher in the vicinity of the SACOC fin as it is found to increase at a steeper rate. Thermal anergy on the other hand is found to be lower than its viscous counterpart, and is mostly generated closer to the SACOC fin. Last, wave anergy losses do not occur in this case because the flow is subsonic.

As for an overall analysis of the impact of the heat exchange itself on the balance, it can be seen that the sum of the anergy components at the SACOC fin level is overall greater than the theoretically-recoverable exergy outflow components downstream of the fin (when considering a reference state at rest). This is particularly the case for the thermocompressible exergy flux term. This estimation alone cannot however provide a definitive conclusion regarding the global effect of a SACOC device on the flow because the terms of the balance are coupled with each other, consistently with the three-dimensional flow physics. It is not therefore straightforward to clearly assess the impact of the heat exchange on the overall performance of a component by only investigating the exergy balance of a single CFD calculation. The contribution of exergy inflow by heat conduction across the non-adiabatic fin surface is not isolated to the Xq term, but also influences the exergy outflow and dissipation components of the balance. A way of more accurately assessing this issue is by performing a comparison against other configurations where the desired level of complexity is progressively introduced.

In particular, a reference computation without SACOC fin is first analysed in order to evaluate a baseline exergy balance of the empty duct. The same mesh topology is kept in order to try to maintain consistency in terms of the baseline numerical losses (see Fig. 1). The solid domain blocks of the SACOC fin are therefore replaced by fluid blocks. The introduction of the viscous effects due to the fin, decoupled from its heat-exchange-associated effects in the non-adiabatic case, consists in analysing a CFD calculation with an adiabatic SACOC fin wall surface. Thermal effects associated to the heat exchange are then added on the same mesh (Fig. 1) by imposing an isothermal boundary condition on the fin. This was carried out by considering increasing, but uniform, wall temperature values. These calculations are compared against the CFD calculation with aerothermal coupling to identify the main impact of the heated wall surface on viscosity, the corresponding thermal effects, and finally the way of introducing the heat exchange itself in the flow (uniform isothermal boundary vs. coupled aero-thermal computation). All these CFD calculations are computed under the same aerodynamic boundary conditions (inlet and outlet) as the coupled aerothermal case of [1]. The

only difference is therefore the boundary condition on the SACOC fin surface (except for the reference duct case where no SACOC fin is present in the duct). The results of the calculation without SACOC fin are, as already mentioned, used as a baseline reference but not included in the following results.

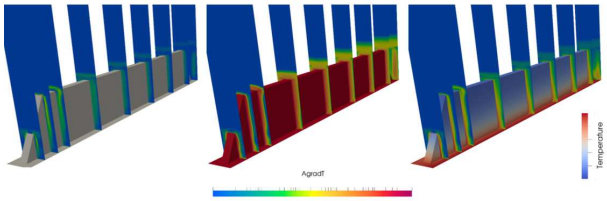


Figure 4: Skin temperature and thermal anergy generation for the isolated SACOC case and different boundary conditions (adiabatic, uniform-temperature isothermal and aerothermal-coupling-based).

The resulting flow field of the calculation shows a flow in axial displacement with a natural development of the boundary layer. The momentum field in Fig. 2 shows that the inlet flow injection is carried out with a head-loaded radial profile. This type of profile is typical of a fan module outlet. The presence of the adiabatic fin introduces viscous effects because it increases the wall viscous surface, obstructs the flow and thus introduces a wake with the presence of vortices at the leading and trailing edges. Fig. 4 shows the growth of the thermal anergy generation component along the SACOC fin.

The impact of different boundary conditions on the SACOC fin surface on some individual exergy balance components is shown in Fig. 5. The consideration of higher wall temperature values leads to the introduction of a higher energy and exergy flux across the SACOC. This is depicted as a change in slope for the Xq component along the fin, except over its inclined leading and trailing edges. Overall, the introduction of the fin increases the viscous anergy by wall friction and vortex generation (horseshoe vortex, vortex due to the oblique edge and downstream fin vortex). Downstream of the fin, after the dissipation of vortex, the viscous anergy slope returns to a natural boundary layer development. It is possible to note that viscous anergy is linked to the thermal boundary layer, as an increased thermal contribution due to the heat exchange is shown to lead to a mild decrease of viscous anergy generation. In addition, the viscous anergy of the aero-thermal coupled computation is found to be in the order of magnitude of the lowest uniform wall temperature value imposed in the isothermal cases. The thermal anergy component is significantly affected by the heat exchange via the SACOC. In the adiabatic case, the introduction of the SACOC fin increases the contribution of the thermal boundary layer and the thermal mixing due to the fin wake, but thermal anergy is of a much lower order of magnitude compared to viscous anergy. Increasing the isothermal fin temperature increases the slope of thermal anergy generation along the fin surface. The integral values eventually become higher than those of viscous anergy, whereas for the higher uniform temperature cases thermal anergy generation even becomes of the same order of magnitude as the main mechanical contributions in the exergy balance. The aero-thermal coupling case leads to an overall thermal anergy value that is intermediate between the two lowest wall temperature values of the isothermal cases. The results also show that a slightly different trend may be obtained for the coupled aero-thermal case compared to the isothermal ones, even though the resulting balance is rather close between the two. The way by which the thermal energy is introduced in the volume is substantially different and so is the generated thermal anergy. As shown in Fig. 4, the thermal anergy fields show that the field around the fin is more homogenous

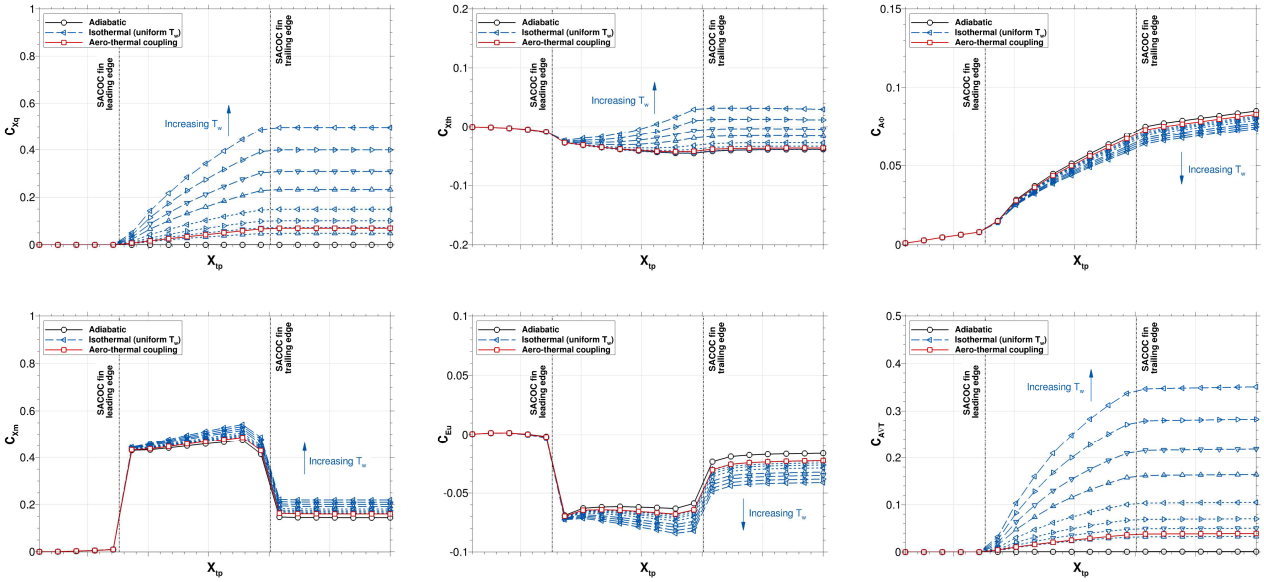


Figure 5: Impact of different boundary conditions (adiabatic wall, isothermal wall at varying uniform wall temperature values, aero-thermal coupling) on components of the exergy balance for the isolated SACOC fin case. The coefficients are adimensionalised by a common reference surface.

in the isothermal case since the temperature is constant. In any case, the wake of the fin undergoes a significant temperature increase due to exchanges with the fin wall and Xth (thermocompressible exergy wasted) exhibits an increase along the inter-fin channel. This is expected to be mainly due to its thermally-recoverable component [14,17]. Concerning mechanical exergy outflow terms, the rate of work of surface forces on the control volume boundary (not shown) increases with a more intense heat exchange. The streamwise perturbation kinetic energy on the other hand shows a decreasing trend with heat exchange, due to the modification of the boundary layer and of the effective passage section in the heated fin cases. The transversal perturbation kinetic energy is only minorly affected in this case. It is also important to note that the influence of the heat exchange on the overall streamwise force (Xtr component, not shown) is minimal and of second order compared to the other mechanical or thermal terms of the balance. Finally, for all of the above cases, the exergy flux (e.g. convertible into useful work) introduced from the heated SACOC surface into the fluid is not the major portion of the overall thermal energy introduced through this heat exchange.

By looking at the global exergy balance, it is possible to observe that a more intense heat exchange leads to a significant increase in thermal exergy introduced into the volume, but at the same time an increase of thermal anergy. A more explicit distinction between the nature of the contribution of the additional exergy inflow could be made by using an adaptation of the formulation for the decomposition of the thermocompressible exergy outflow [14,17]. Although this is not investigated in the present work, the additional contribution is expected to only be thermally-recoverable by a heat engine and not mechanically-recoverable by a turbine or a nozzle (cf. also similar studies in [19]). Still, in the present case, the increase in thermal anergy has been found to be greater than the increase in thermocompressible exergy outflow. This means that the SACOC introduces thermal exergy of poor quality that is quickly dissipated by thermal mixing and therefore not easily usable by the system. It is however possible that more advanced fin geometries leading to reduced fluid mixing could reduce this thermal anergy generation. Furthermore, thermal anergy surpasses viscous anergy and becomes the main source of irreversible exergy loss for the cases of higher wall temperature.

Another conclusion from the comparison of the analysed cases is that it is unlikely that uniform-temperature isothermal computations can quantitatively reproduce the flow details of a coupled aerothermal calculation. However, qualitative comparisons can be acceptable. In order perform such comparisons, it is necessary to choose the analogy of the comparison; therefore, to choose whether to compare the coupled aerothermal calculation with an isothermal calculation considering the same amount of thermal energy or exergy introduced into the fluid by the exchanger, or the same anergy generation due to thermal mixing. For a similar amount of energy inflow, a coupled aerothermal calculation creates slightly less thermal anergy. In terms of thermal anergy generation, the coupled aerothermal case gives a slightly higher prediction than the isothermal calculation at the lowest temperature and therefore with the least introduction of heat into the system among the considered cases.

## 3.2. Isolated SACOC fin array

Ideally, the performance of a SACOC should always be evaluated within its operational context, such as a turbofan engine. However, due to cost and time constraints, smaller-scale tests and simulations remain essential. Therefore, wind tunnel testing remains a common approach for such analyses. It is crucial to gauge how well such experimental setups mimic real engine conditions. This necessity drove the development of the second SACOC configuration presented in this study.

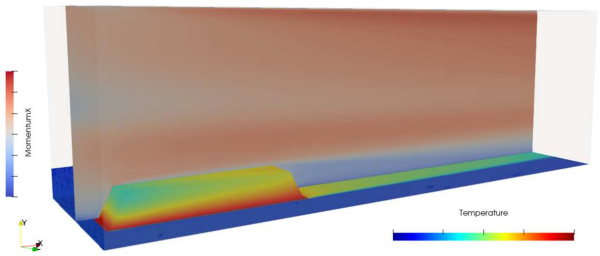


Figure 6: Sixteen SACOC fin array: streamwise momentum velocity and temperature on the skin.

The heat exchanger configuration of the sixteen SACOC fins aims at reproducing a wind-tunnel test configuration. An illustration of the case geometry and flow field is shown in Fig. 6. It includes a channel with four adiabatic walls, sixteen SACOC fins with a boundary condition resulting from an aero-thermal coupling, a 2D map injection at the inlet, and a static pressure boundary condition at the outlet. The sixteen fins are placed on the lower wall of the wind tunnel at the same distance from the inlet as the one separating the SACOC and the OGV/BPD interface in a real engine configuration (see Fig. 9 and the study of the following section). The 2D map injected at the inlet is extracted from a fan/OGV computation and portrays the wake of an OGV. The particular interest of this configuration is to analyse how the wake of the OGV interacts with the SACOC fins and how this interaction could affect the heat exchange.

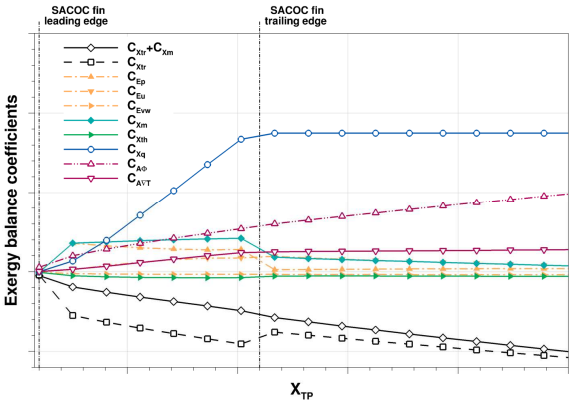


Figure 7: Evolution of the exergy balance for a variation of the control volume's downstream limit in the sixteen SACOC fin array case.

In the exergy balance of the SACOC fin array in a wind-tunnel test section (shown in Fig. 7), a stronger coupling of mechanical (e.g. pressure-related) and thermal terms is observed. The thermal exergy introduced by the fins into the fluid (Xq) represents a significant contribution amongst the rest of the exergy balance components. This exergy introduced is monotonically increasing but not always linearly, in particular in the regions of the inclined leading and trailing edges of the fins. The viscous and thermal anergy components of the balance increase at the level of the fins (with the former being of a larger magnitude) but also further downstream due to: shear from the injected OGV wake at the inlet, thickening of the boundary layer on all walls, the presence of vortices and compression effects in the test section. As in the case of the previous section (aerothermal coupling), the increase of thermal anergy downstream of the SACOC is less significant than the increase of viscous anergy. It is finally interesting to note the variations of mechanical exergy outflow components (streamwise and transversal perturbation kinetic energy) in the vicinity of the fins. The overall behaviour of the different components of the exergy balance is found to be similar to that in the isolated SACOC fin configurations of the previous sections, although the relative magnitude of some components is different due to this section being based on a more complete geometry and more realistic heat exchange considerations. Finally, Fig. 8 illustrates the higher fidelity of the present configuration, in particular due to the interaction of the SACOC with the fan/OGV wake.

The comparison between the isolated fin and the sixteen-fin array SACOC configurations highlights the intricate interplay between thermal and mechanical physics. Optimizing a SACOC in an idealized environment might overlook these complex interactions, as the reality of aircraft engine installations presents a vastly different scenario. In such installations, the SACOC operates within a dynamic and tightly integrated system, where thermal and mechanical effects are closely intertwined. This coupling requires a more comprehensive approach to design and optimization, considering the realistic operational condition constraints and interactions inherent in engine installations. A step towards such conditions is made in the study of the following section.

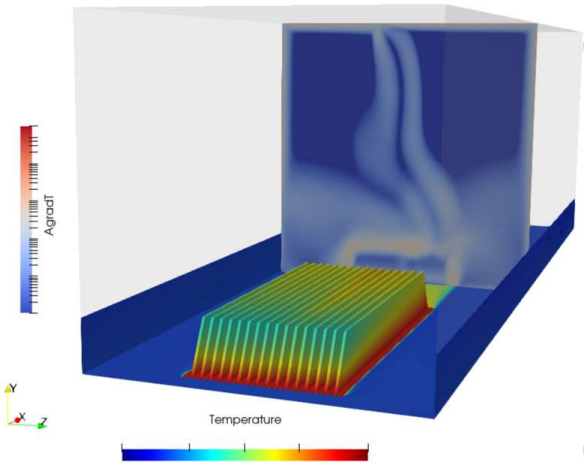


Figure 8: Sixteen SACOC fin configuration: surface temperature and thermal anergy generation.

### 3.3. FAN-OGV-SACOC in a BPD

The turbofan configuration of this section aims at replicating real-world engine operating conditions, crucial for understanding the performance of a SACOC [1,16]. Installed on the outer fixed structure (OFS) of a turbofan bypass duct (BPD), the SACOC consists of 50 fins of a similar geometry as those studied in the previous sections. Positioned slightly downstream of the OGV, this setup mimics the operational environment. The configuration corresponds to a fan composed of 18 blades and an OGV composed of 40 (homogeneous) blades. The fluid domain represents an angular sector of the BPD, encompassing one fan and one OGV blade. This fluid domain, discretized with a grid of around 73 million nodes (particularly refined in the SACOC region), spans downstream from the fan inlet up to the primary stream intake and then up to the outlet at the throat of the nozzle. It is divided into three sub-domains. The fan sub-domain extends over 20°, from the inlet to the interface with the OGV sub-domain, and the fan operates under standard conditions with the steady flow solution being computed in a rotating reference frame. The OGV sub-domain extends over 9°, from the interface with the fan sub-domain to the inlet of the BPD. The fan and OGV blade surfaces are modelled as adiabatic no-slip walls. A mixing-plane boundary allows communication between the rotor and stator, introducing some homogenization into the flow while preserving radial gradients. The BPD sub-domain extends for 9°, from the interface with the OGV sub-

domain to the nozzle outlet. It includes a mismatched connectivity at the boundary between the OGV and BPD sub-domains, as well as the aero-thermally coupled SACOC surface with a prescribed temperature boundary condition resulting from the coupling itself. An adiabatic no-slip condition applies to the remaining wall surfaces, with a pressure boundary condition prescribed at the nozzle outlet. This configuration allows for the consideration of various aspects of realistic turbofan operation, including aerodynamic interactions between the SACOC and OGV, the heat exchange impact on engine thrust, and more realistic flow conditions at the SACOC fins. Due to these considerations, this consists in one of the most physically and geometrically complex configurations so far studied with the exergy balance method.

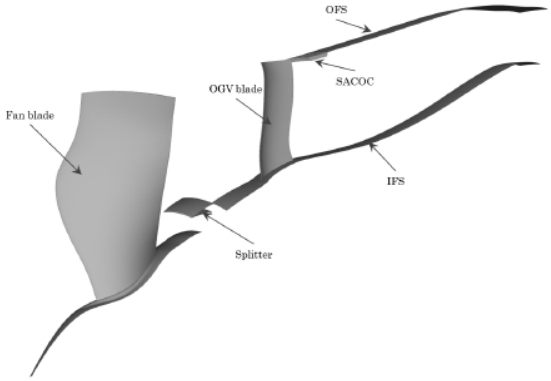


Figure 9: Three-dimensional view of the computational domain of the Fan-OGV-SACOC-BPD case [16].

In the fan sub-domain, the computed exergy balance is projected in the rotating frame of reference attached to the fan blades [14]. The formulation naturally degrades to its inertial frame counterpart in non-rotating sub-domains, thus allowing the simultaneous treatment of rotating and non-rotating domains in the present test case. Solutions of this level of complexity can therefore be straightforwardly treated in a uniform manner using the formulation implemented in the FFX analysis software. In such cases, the computed exergy balance corresponds to the complete 360° configuration in order to ensure consistency across the mixing-plane interface. On the other hand, since consistency is ensured at the formulation and numerical level, it is also possible to carry out a modular analysis of the fan and of the OGV-SACOC-BPD parts, which provides significant flexibility in practical studies of complex systems.

The variation of the exergy balance along the engine axis is shown in Fig. 10. The numerical implementation of the formulation ensures that the balance is consistent across the mixing-plane and mismatched connectivity boundaries. The rotating fan introduces a significant amount of mechanical exergy into the flow, which is depicted in the Xr term of the exergy balance (not shown). Results show that the increased transversal kinetic perturbation exergy flux (Evw) introduced into the fluid by the fan is greatly reduced across the OGV, which is translated to an increase of overall streamwise force (Xtr, i.e. thrust). The evolution of the overall mechanical exergy flux (Xm) underlines the non-negligible contributions from its other two components (axial kinetic perturbation exergy flux and rate of work of surface forces). Overall, the (theoretically-recoverable) mechanical exergy outflow is shown to be more significant than irreversible exergy losses in this case. The influence of the SACOC is of a much lower magnitude than the fan and OGV contributions, but quantifiable with good accuracy. Fig. 10 also shows a detail of anergy generation components and energy/exergy flux into the fluid through conduction across the SACOC surface. This shows that only a small portion of the introduced thermal energy is theoretically convertible into useful work. Furthermore, these results highlight the decomposition of irreversible losses of exergy (anergy generation) into different components. Thermal anergy is of a generally lower magnitude but exhibits an increase in the SACOC region where temperature gradients are the strongest. In the fan region, viscous and wave anergy losses are roughly similar at this operating point of the engine. Further downstream, wave anergy only shows a minor increase due to a lower-intensity shockwave at the OGV, whereas viscous anergy continues to increase due to the presence of strong viscous effects (boundary layers, wakes, generation and diffusion of vortices).

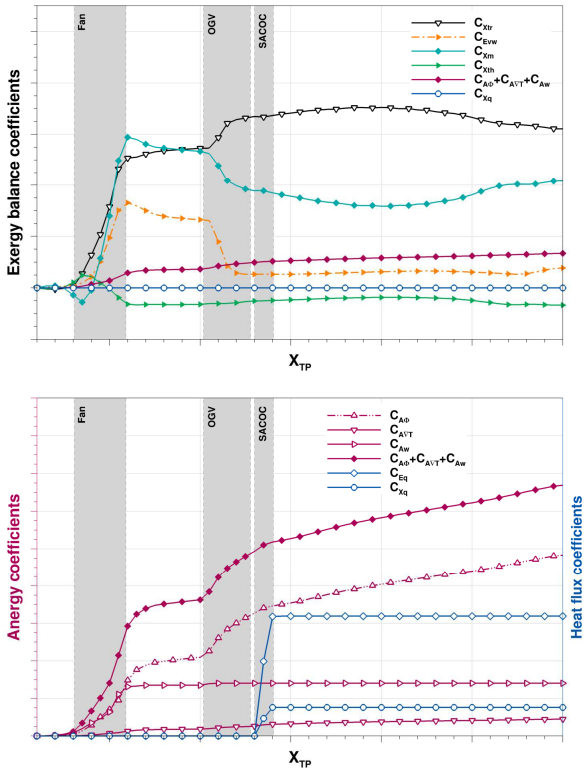


Figure 10: Evolution of the exergy balance along the engine axis in the fan-OGV-SACOC-BPD case.

An interesting advantage of the exergy balance method is the possibility of visualizing the corresponding anergy generation or exergy flux fields in order to refine the interpretation of integral results and their association to individual physical phenomena occurring in the flow. Straightforward assessments of this type are not always possible with classical performance metrics.

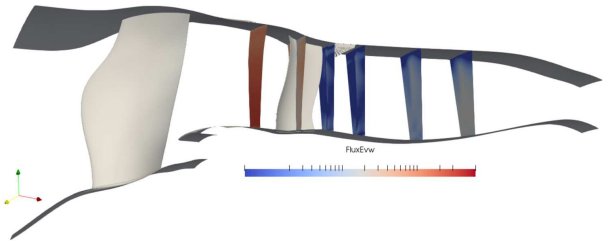


Figure 11: Transversal perturbation kinetic energy at different axial positions in the fan-OGV-SACOC-BPD configuration.

Fig. 11 shows the transverse perturbation kinetic energy flux, showing the areas where the OGV exhibits a lack of optimal efficiency. More specifically, higher Evw flux values are present in a zone near the SACOC, due to the presence of the SACOC itself, but also a central zone and one at the foot of the OGV. This OGV profile thus has room for improvement in design for this particular operating point. This is consistent with the non-zero integral value of perturbation kinetic energy flux Evw downstream of the OGV (cf. Fig. 10).

Fig. 12 then illustrates the generation of thermal anergy at different axial positions in the OGV-SACOC region. These visualisations show that this component is more significant in the boundary layers (the fan wake having been smeared azimuthally across the mixing plane boundary) and the wake of the OGV, while further downstream it is especially the case in the vicinity of the SACOC due to the intense heat exchange in this region. The visualization of the viscous anergy field in Fig. 13 accurately depicts the trace of the shockwave upstream of the fan and the thickening of the boundary layer on the fan blade. As expected, the highest values of viscous anergy generation are shown to be concentrated in the boundary layers and wakes. The wake of the fan blade is reintroduced by injection on the OGV/secondary stream after an azimuthal averaging across the mixing plane. No significant effects of the mixing-plane approximation were however identified across the fan/OGV interface in terms of the overall exergy balance (cf. Fig. 10), showing that integral values are accurately preserved despite the azimuthal averaging.

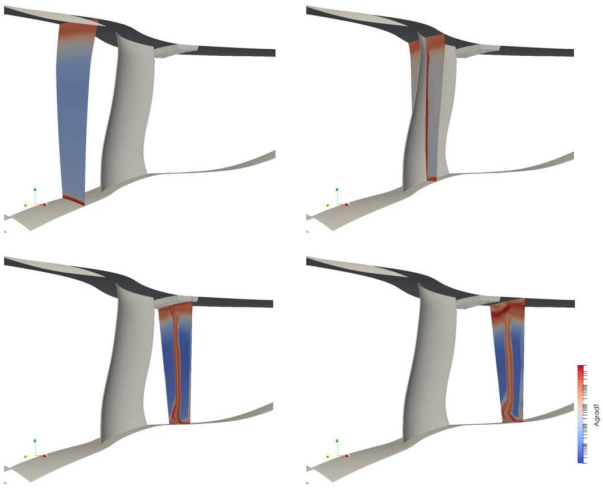

Figure 12: Thermal anergy generation at different axial positions in the OGV-SACOC region of the fan-OGV-SACOC-BPD configuration.

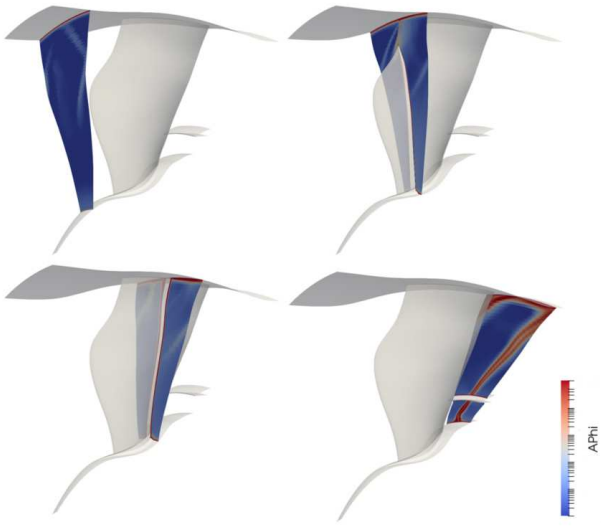


Figure 13: Viscous anergy generation at different axial positions in the fan region of the fan-OGV-SACOC-BPD configuration.

The main conclusion of the exergy analysis for the FAN-OGV-SACOC/BPD case confirms the observations for the sixteen SACOC case: consistent exergy balance results were obtained across the configurations of increasing complexity but the study highlights the complex relationship between thermal and mechanical physics. This becomes even more important in realistic transonic operating conditions, where compressible effects are also significant. Simply optimizing a SACOC in a controlled setting might neglect these intricate dynamics. The environment of aircraft engine installations should therefore be considered for a complete design and optimization strategy.

## 4. CONCLUSIONS

This paper has consisted in the use of the exergy balance method to analyse SACOC heat exchanger devices for civil aircraft engines. In particular, configurations of progressively-increasing complexity were considered in order to assess the consistency of results when the level of complexity ranges from simplified design studies to the more realistic operating conditions of an integrated device. The results obtained during this study overall show that the thermal energy introduced by a SACOC into the fluid is not of high quality, in the sense that the introduced exergy can be quickly dissipated by thermal mixing. The increasing isothermal (uniform temperature) cases in the isolated SACOC fin study show an increase in the energy and exergy inflow level into the flow, but ways of converting this energy into effective trust are limited in practice. The exergy balance of the more complex cases (sixteen SACOC fins and FAN-OGV-SACOC) suggests the same conclusion, although additional reference cases would be needed for comparison in order to more accurately quantify these effects. Still, the employed exergy balance methodology has been found to give a fine decomposition and an accurate quantification of the effects introduced into the flow by a SACOC, even if these effects are of a significantly lower magnitude than the main flow physics (e.g. when integrated downstream of a fan module). Alternative integration methods for these devices can also be considered in order to identify those leading to lower losses due to thermal mixing. As a perspective of this study, it would be particularly interesting to extend this analysis to different operating and atmospheric (and therefore thermodynamic) conditions across the flight envelope in order to identify points where the SACOC can have a more favourable impact on the flow, in particular with respect to the eventual recovery of the thermal exergy introduced by the heat exchange. Recently-proposed refinements of the formulation may improve these analyses in terms of more straightforwardly targeting the mechanically- or thermally-recoverable parts of the exergy flux [14,17].

The present study is part of a wider-spectrum investigation of the exergy balance method within the IDEFFIX research project, in configurations of industrial interest and complexity. Across these studies, the exergy balance method has shown to be mature enough to accurately quantify the impact of individual effects on overall performance in order to provide a reliable physical insight to designers of complex industrial configurations. In conclusion, this project represents a significant contribution to aerodynamic research, offering a physically-refined perspective for the aviation industry in terms of performance assessment based on the analysis of flow solutions. The exergy balance formulation stands as an indispensable tool for addressing future challenges in aviation, reconciling increased performance with enhanced environmental respect, in terms of both aerodynamics and multidisciplinary aero-thermal interactions.

## ACKNOWLEDGEMENTS

The IDEFFIX (Industrial Development of Far-Field Exergy) research project was co-funded by the French Directorate General for Civil Aviation (DGAC) in the frame of the French national Plan de relance, supported by European Union funding within the NextGeneration EU framework. The CFD computations presented in this work were carried out with the elsA solver, whose development is partially funded by its co-owners, ONERA and Safran.

## REFERENCES

1. Gelain, M., “Aerothermal characterisation of a surface heat exchanger implemented in a turbofan by-pass duct”, Doctoral dissertation, Université Paris-Saclay, 2021.
2. CFM International RISE (accessed on 7/3/2024), https://www.cfmaeroengines.com/rise/.
3. Arntz A., Atinault O. and Merlen A., “Exergy-based formulation for aircraft aeropropulsive performance assessment: theoretical development”, *AIAA Journal*, Vol. 53, No. 6, 2015, pp. 1627-1639, DOI: 10.2514/1.J053467.
4. Berhouni I., Bailly D. and Petropoulos I., “On the definition of exergy in the field of aerodynamics”, *AIAA Journal*, Vol. 61, No. 10, 2023, pp. 4356-4366, DOI: 10.2514/1.J062833.
5. Bajusz, D., Cornet, A., Friedel, J., and Raimarckers, N. Air-oil heat exchanger placed at the location of the air separator nose of a turbojet, and a turbojet including such an air-oil heat exchanger, July 2 2009. US Patent App. 12/342,206
6. Kim, M., Ha, M. Y., and Min, J. K. A numerical study on various pin–fin shaped surface air–oil heat exchangers for an aero gas-turbine engine. *International Journal of Heat and Mass Transfer*, 93:637–652, 2016.
7. Kim, S., Min, J. K., Ha, M. Y., and Son, C. Investigation of high-speed bypass effect on the performance of the surface air–oil heat exchanger for an aero engine. *International Journal of Heat and Mass Transfer*, 77:321–334, 2014.
8. Sousa, J., Villafañe, L., and Paniagua, G. Thermal analysis and modeling of surface heat exchangers operating in the transonic regime. Energy, 64:961–969, 2014.
9. Villafañe, L. and Paniagua, G. Aerodynamic impact of finned heat exchangers on transonic flows. *Experimental Thermal and Fluid Science*, 97:223–236, 2018
10. Manglik, R. M. and Bergles, A. E. Heat transfer and pressure drop correlations for the rectangular offset strip fin compact heat exchanger.

*Experimental Thermal and Fluid Science*, 10(2):171–180, 1995.

11. Sparrow, E., Baliga, B., and Patankar, S. Forced convection heat transfer from a shrouded fin array with and without tip clearance. *ASME Journal of Heat Transfer*, 100:572–579, 1978.
12. Tadeusz J. Kotas. The Exergy Method of Thermal Plant Analysis, Chapter 4 - *Exergy analysis of simple processes*. Elsevier, 1985.
13. Garaud, J., Rannou, J., Bovet, C., Feld-Payet, S., Chiaruttini, V., Marchand, B., Lacourt, L., Yastrebov, V., Osipov, N., and Quilici, S. Z-set-suite logicielle pour la simulation des matériaux et structures. In 14ème Colloque National en Calcul des Structures, 2019.
14. Berhouni I., Theoretical study of the exergy balance method and extension to the performance analysis of steady rotating flows. PhD thesis, Institut Polytechnique de Paris, France, 2023. NNT: 2023IPPAX131.
15. Petropoulos I., Bailly D. and Berhouni I. Development of numerical accuracy indicators for the far-field exergy balance method. In AIAA Aviation Forum 2023, Paper 2023-3389, DOI: 10.2514/6.2023-3389.
16. Gelain, M. C., Couilleaux, A., Errera, M., Vicquelin, R., & Gicquel, O. (2021). Conjugate heat transfer analysis of a surface air-cooled oil cooler (SACOC) installed in a turbofan by-pass duct. In AIAA Aviation 2021 Forum (p. 3163).
17. Berhouni I., Bailly D. and Petropoulos I., Exergy Balance Decomposition Between Mechanically- and Thermally-Recoverable Exergy Outflows, AIAA Journal, Vol. 62, No. 3 (2024), pp. 1232-1239, DOI: 10.2514/1.J063118.
18. Cambier, L., Heib, S., and Plot, S., The Onera elsA CFD software: input from research and feedback from industry, Mechanics & Industry, 14(3):159–174, 2013. DOI:10.1051/meca/2013056.
19. Morelli M., Trapier S., Lopez de Vega L., Thollet W., Petropoulos I., Berhouni I., Assessment of the Far-Field Exergy Balance Method for Industrial Aerodynamic and Aerothermal Applications, Paper AERO2024-37, 58th 3AF International Conference on Applied Aerodynamics, Orléans, France, March 2024.
20. Petropoulos, I., Bailly, D, Atinault, O., Hantrais-Gervois, J.-L., Wervaecke, C., Boniface, J.-C., Dumont, A., Berhouni, I., Trapier, S., Morelli, M., Lopez de Vega, L., Thollet, W., Paladini, E., and Couilleaux, A., Overview of the IDEFFIX project towards the development of the far-field exergy balance method at an industrial level of complexity. In 58th 3AF International Conference on Applied Aerodynamics, Orléans, France, 27-29 March 2024. Paper ID: AERO2024-15.